

Technical Note

SEISMICITY OF ZARAND REGION AT SOUTH EAST OF IRAN

H. Ghasemi, F. Sinaeian, A. Beitollahi and H. Mirzaei
Building and Housing Research Center, Tehran, I.R. Iran

ABSTRACT

In order to study the seismicity of Zarand region at south east of Iran, 27 accelerograms obtained during the main-shock of 2005 Dahooeyeh-Zarand earthquake are used. For this purpose, the local magnitude (M_L) and attenuation parameters of the region (shear waves quality factor and kappa) are determined.

The frequency dependency of quality factor, Q_β , and the S-wave high-frequency spectral-decay parameter, κ (a measure of wave attenuation), on epicentral distance are studied.

Keywords: seismicity, local magnitude, spectral decay parameter, quality factor, Dahooeyeh-Zarand earthquake

1. INTRODUCTION

At 2:25:26 GMT (5:55:26 Local time) on 22 Feb. 2005 an earthquake with the magnitude of M_w 6.3 struck Zarand region in Kerman province. Based on the information obtained, few villages either totally destroyed, or underwent some damages. In the struck region there are about 15000 people inhabits and buildings are in different types, from old sun-dried mud-brick and mud to modern type with still structures and concrete. But damaged types commonly could be categorized in the first type. The earthquake caused extended damage in Dahooeyeh and Hotkan villages which are totally destroyed and left more than 600 deaths while the injured reached more than 1000.

The studied area has experienced many moderate to strong earthquakes, which had been left many deaths and devastations. In this regard we can mention Horjand earthquake ($M_S=5.8$) on Nov. 1854, Chatrood earthquake ($M_S=6.0$) on Jan. 1864. The last earthquake before the studied event took place on Dec.1977 with the magnitude $M_S=5.7$ left more than 660 deaths.

The main-shock of this earthquake triggered 27 accelerographs in the radius of about 240 Km of the epicenter (Figure 1). The maximum peak ground acceleration as much as 510.09 gals was recorded at the Shirinrood Dam station. The epicenter of the earthquake has been

located at 30.804N, 56.734E (BHRC*).

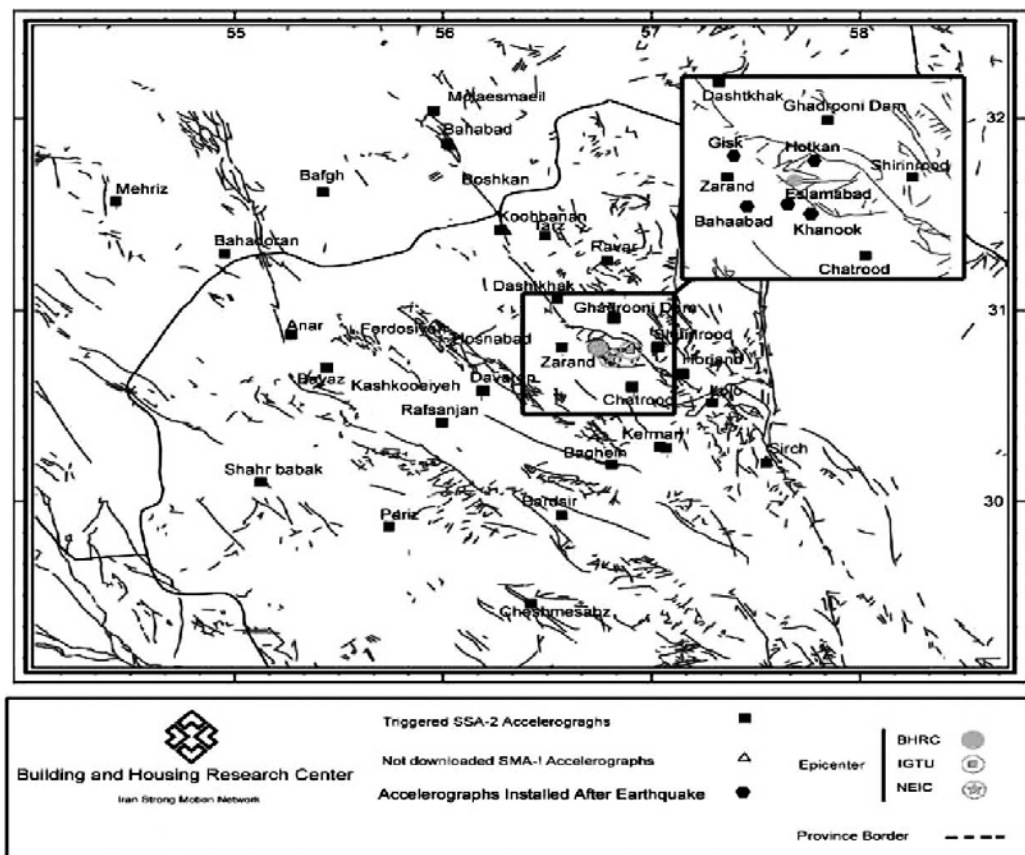


Figure 1. The main tectonic features of the studied area nearby the triggered stations during the main-shock of the 2005 Dahooeyeh-Zarand earthquake [bhrc].

In the present study the attenuation parameters, Quality factor and Spectral decay parameter, nearby the local magnitude scale are investigated using obtained accelerographs during the main-shock of 2005 Dahooeyeh-Zarand earthquake.

The local magnitude is based on the amplitude recorded by the wood–Anderson torsion seismograph with the definite specifications. It has the most relevance to engineering applications, because M_L is determined within the period range of greatest engineering interest. The magnitude is estimated from every seismograph station that has been triggered and to minimize the station site effects, the mean value is calculated [5].

Attenuation of seismic wave amplitudes can be considered due to two main processes: Elastic processes (e.g. geometrical spreading) and inelastic processes (e.g. intrinsic attenuation) and often can be discussed in terms of Q and Q^{-1} which are proportional with

* Building and Housing Research Center

damping [1]. In seismology we speak of the Q of surface waves, body waves and crustal phases (e.g. L_g). From engineering point of view shear waves quality factor, Q_β investigated in the present study, has more importance than others because of the amplitude and frequency content of shear waves. Based on the obtained results the Q_β for S-waves increases with frequency and propose frequency dependant quality factor as $Q=138f^{0.81}$, implies the high activity of the region. Spectral decay parameter, also determined in the present study, is used to determine the shape of high frequency portion of acceleration spectra [2].

The exact physical process caused the observable decay trend in high frequency portion of acceleration spectra is somewhat unknown; It may be due to source or site effects nevertheless, it can be quantified by determining so called Kappa parameter [2]. Kappa parameter has a great importance in engineering applications. For example it can be considered as a clue for sediments nonlinearity behavior during an earthquake [3] or can be used in some models to simulate strong motions, etc.

2. DATA SET FOR THE PRESENT STUDY

The original data set used in the present study includes the 2005 Dahooeyeh-Zarand event contained in the BHRC database. 54 horizontal accelerograph components are used, obtained from 27, three-component stations which their characteristics summarized in Table 1.

The recording instruments are digital accelerographs (Kinematics SSA-2) were installed at distances ranging from 17 to 236 km with respect to the epicenter of the examined earthquake.

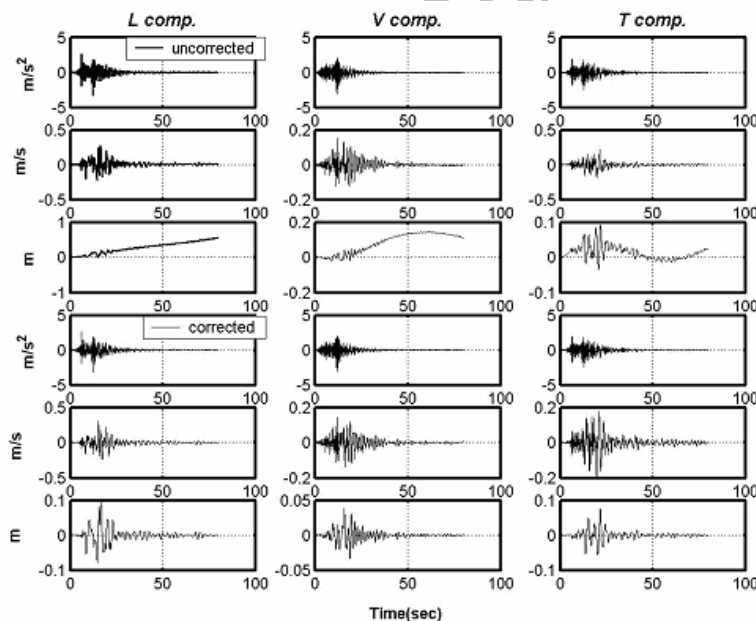


Figure 2. The uncorrected (up 3 rows) and corrected (down 3 rows) acceleration, velocity and displacement time histories for Zarand station.

The baseline correction and removing the instrumental response carried out on digital waveforms following a standard procedure similar to Ref. [4], then they band pass filtered in the frequency range in which the signal to noise ratio was equal to or greater than 3 using a fourth-order Butterworth filter. Figure 2 shows the uncorrected and corrected waveforms recorded at Anar station with peak ground acceleration equals to 510.09m/s/s and 202.55m/s/s on horizontal components (L&T), respectively.

Table 1. Characteristics of the used strong motion records nearby the estimated spectral decay parameter values at each station

Station	Coordinates		Altitude (m)	Azimuth of accelerographs		ED (Km)	Corrected PGA (g)			Spectral decay parameter (Kappa)		
	E	N		L	T		L	V	T	L	T	Ave
Zarand	56.57	30.81	1678	34	124	17	0.32	0.31	0.25	0.050	0.052	0.025
Qadrooni Dam	56.82	30.96	1665	170	260	19	0.22	0.11	0.14	0.052	0.056	0.026
Shirinrood Dam	57.03	30.81	1788	95	185	27	0.50	0.25	0.20	0.030	0.031	0.015
Chatrood	56.91	30.60	1841	60	150	28	0.06	0.06	0.09	0.040	0.050	0.020
Dasht-e Khak	56.55	31.06	2226	210	300	34	0.05	0.05	0.06	0.071	0.067	0.035
Horjand	57.15	30.67	2320	0	90	41	0.05	0.07	0.04	0.096	0.074	0.048
Ravar	56.79	31.26	1244	320	50	51	0.12	0.04	0.07	0.083	0.077	0.042
Davaran	56.19	30.58	1860	135	225	59	0.06	0.03	0.05	0.049	0.040	0.025
Deh- Loulou	57.29	30.52	2069	150	240	61	0.05	0.02	0.03	0.067	0.092	0.033
Kerman 1	57.04	30.29	1767	170	260	64	0.03	0.02	0.03	0.083	0.064	0.041
Kerman 2	57.07	30.28	1755	147	237	66	0.03	0.02	0.03	0.083	0.078	0.041
Baghin	56.81	30.19	1718	100	190	69	0.03	0.02	0.02	0.106	0.094	0.053
Tarz	56.49	31.39	1820	158	248	70	0.03	0.02	0.04	0.116	0.110	0.058
Koohbana n	56.27	31.42	2008	170	260	82	0.01	0.01	0.01	0.078	0.083	0.039
Rafsanjan	55.99	30.41	1520	340	70	85	0.02	0.01	0.02	0.080	0.109	0.040
Bardsir	56.57	29.92	2113	75	165	100	0.01	0.01	0.01	0.137	0.103	0.068
Sirch	57.55	30.20	1685	30	120	102	0.01	0.01	0.01	0.071	0.085	0.035
Bayaz	55.44	30.70	1453	140	230	125	0.01	0.01	0.01	0.082	0.088	0.041
Bahabad	56.02	31.87	1373	160	250	137	0.01	0.01	0.02	0.090	0.090	0.045
Anar	55.27	30.87	1423	24	114	141	0.02	0.01	0.01	0.094	0.084	0.047
Pariz	55.74	29.87	2325	10	100	142	0.01	0.01	0.01	0.089	0.099	0.044
Cheshmeh sabz	56.42	29.46	2581	65	155	153	0.01	0.00	0.01	0.103	0.114	0.051
Bafgh	55.42	31.62	951	102	192	155	0.01	0.01	0.01	0.092	0.091	0.046
Molea Esmaeel	55.95	32.04	1346	310	40	157	0.01	0.01	0.02	0.109	0.106	0.054
Shahre Babak	55.12	30.10	1840	86	176	174	0.01	0.01	0.02	0.089	0.102	0.045
Bahadoran	54.95	31.30	1460	135	225	180	0.01	0.01	0.02	0.062	0.103	0.031
Mehriz	54.43	31.57	1480	320	50	236	0.01	0.00	0.01	0.169	0.174	0.084

3. METHODS FOR THE CALCULATION OF SEISMICITY PARAMETERS

3.1 Local Magnitude

The local magnitude is based on the amplitude recorded by the Wood-Anderson torsion seismograph with a natural period of 0.8 sec, a damping constant of $h=0.8$ and a static magnification, $Y=2800$. Among the several magnitude scales in current use, the local magnitude (M_L), introduced by Richter [8], has the most relevance to engineering applications, because M_L is determined within the period range of greatest engineering interest [5-6].

The Wood-Anderson response A_j , is computed using the following equation, which corresponds to the differential equation for the Wood-Anderson response to acceleration input a_j :

$$A_j = 1/C_2 [g_{wa} \Delta t^2 a_j + 2C_1 A_{j-1} - A_{j-2}] \quad (1)$$

where

$$C_1 = 1 + h\omega_0 \Delta t \quad , \quad C_2 = 1 + 2h\omega_0 \Delta t + (\omega_0 \Delta t)^2$$

h , ω_0 and g_{wa} are the damping constant, natural angular frequency, and the gain factor of the Wood-Anderson instrument, respectively [7].

In order to calculate the M_L using A_j , we used equation (2), used by Richter in southern California:

$$M_L(j) = \text{LoG}_{10} A_j(\text{mm}) + 3\text{LoG}_{10}(8\Delta t(\text{s})) - 2.92 \quad (2)$$

here A_j (mm) is the Wood-Anderson response to acceleration input a_j in millimeters, and the S-P time, in seconds, makes $\Delta t(\text{s})$ in seconds [8] for event j .

Seismologists try to get a separate magnitude estimate from every seismograph station that records the earthquake and then average them. We do the same for each accelerograph station that records the event and then average them.

No station corrections were included in the computations of M_L , but station effects thought to be minimized when the average is taken [5].

The results of M_L computation of the Dahoeiyeh-Zarand earthquake are presented in Table 2.

3.2 Quality factor

To determine quality factor of shear waves, Q_β , the method described in Ref. [9-12] is followed, in which the decay trend of the observation with distance, due to geometrical spreading, scattering and absorption, described as:

$$A(f, R) = G(R) e^{-\pi f / Q_\beta} \quad (3)$$

where $G(R)$ is the geometrical spreading function, f is the frequency and t is the travel time. For body waves $G(R)$ can be approximated as $1/R$ for short distances, (R being the hypocentral distance) which implies spherical geometry.

Table 2. Local Magnitude M_L for the Dahooiyeh-Zarand earthquake determined from strong-motion accelerograms.

Station	Record No.	Station		S-P (Sec.)	ED (Km.)	M_L			
		Lat.	Lon.			1	2	3	4
Qadrooni Dam	3689-1	30.96	56.82	3.61	19	5.7	5.2	5.3	5.4
Zarand	3671-1	30.81	56.57	4.63	17	6.3	5.4	6.1	5.7
Shirinrood Dam	3697-1	30.81	57.03	4.62	27	6.2	5.3	4.8	5.6
Chatrood	3660-1	30.60	56.91	5.14	28	5.9	5.5	5.0	4.9
Dasht-e-Khak	3686	31.06	56.55	5.40	34	5.7	5.8	5.8	5.7
Horjand	3688	30.67	57.15	6.07	41	6.0	5.7	5.2	5.5
Deh-Loulou	3679	30.52	57.29	8.01	61	6.2	5.9	5.8	5.9
Ravar	3661	31.26	56.79	8.03	51	6.5	6.1	6.3	6.3
Kerman 1	3662	30.29	57.04	8.56	64	6.5	6.2	6.2	6.2
Kerman 2	3687	30.28	57.07	9.10	66	6.4	6.4	6.1	6.1
Baghin	3663	30.19	56.81	9.79	69	6.3	6.3	6.1	6.0
Tarz	3665	31.39	56.49	9.83	70	6.4	6.2	6.4	6.4
Rafsanjan	3673	30.41	55.99	10.31	85	6.5	6.2	6.7	6.5
Sirch	3672	30.20	57.55	12.18	102	6.2	6.3	6.1	6.1
Davaran	3702	30.58	56.19	*	59	*	6.2	6.0	5.8
Koohbanan	3677	31.42	56.27	*	82	*	6.1	6.3	6.2
Bardsir	3667	29.92	56.57	*	100	*	6.3	6.4	6.3
Bayaz	3670	30.70	55.44	*	125	*	6.5	6.6	6.5
Bahabad	3669	31.87	56.02	*	137	*	6.6	7.0	7.0
Anar	3674	30.87	55.27	*	141	*	6.5	6.7	6.6
Pariz	3684	29.87	55.74	*	142	*	6.7	6.3	6.2
Cheshmeh sabz	3675	29.46	56.42	*	153	*	6.9	6.5	6.5
Bafgh	3668	31.62	55.42	*	155	*	6.9	7.0	7.0
Molea Esmaeel	3678	32.04	55.95	*	156	*	7.0	7.3	7.3
ShahreBabak	3685	30.10	55.12	*	174	*	7.1	6.9	6.8
Bahadoran	3666	31.30	54.95	*	180	*	7.1	7.3	7.2
Mehriz	3664	31.57	54.43	*	236	*	6.1	7.3	7.3
Mean						6.2	6.2	6.2	6.2
SD						0.29	0.58	0.67	0.60

1. S-P is used for M_L

2. Epicenter of Building and Housing Research Center (BHRC) is used

3. Epicenter of Institute of Geophysics of Tehran University(IGTU) is Used

4. Epicenter of United States Geological Survey(USGS) is used

The second phrase in Eq. (3) represents the exponential decay of the amplitudes caused by scattering and absorption of seismic waves traveling in the earth.

Substituting $G(R)$ as $1/R$ and taking logarithm from Eq. (3) we have

$$\text{Log}(A(f, R)) = -\text{Log}(R) - \text{Log}(e) \frac{\pi f R}{Q_\beta V_s} \quad (4)$$

where V_s is the shear wave velocity taken as 3.5 Km/s for shear waves.

In the nonparametric approach described in Ref. [13] the observed spectral amplitudes, $u_i(f, R)$ for a fixed frequency f at hypocentral distance R from the earthquake i can be modeled as:

$$u_i(f, R) = S_i(f) \cdot A(f, R) \quad (5)$$

where $S(f)$ is a scalar which depends on the size of the earthquake and $A(f, R)$ is the attenuation function described as Eq. (3). Substituting Eq.(4) to Eq.(5) gives:

$$\text{Log}u_i(f, R) + \text{Log}R = \text{Log}S_i(f) - \pi \text{Log}(e) \frac{f}{\beta Q_\beta} R \quad (6)$$

According to Eq. (6) after correcting the spectral amplitudes against geometrical spreading, the slope of the least square fitted line (b) between $\log u_i(f, R) + n \log R$ and R must be proportional to Q_β through equation:

$$b = -\pi \text{Log}(e) \frac{f}{\beta Q_\beta} \quad (7)$$

or equivalently:

$$Q_\beta = \frac{-\pi \text{Log}(e) f}{b \beta} \quad (8)$$

gives the Q_β value for the fixed frequency f .

By calculating Q_β for several frequencies using above method, we can determine the functional form of the frequency dependant quality factor described as

$$Q = Q_0 f^\alpha \quad (9)$$

where Q_0 and n are constants.

3.3 Spectral decay parameter

To determine the spectral decay parameter, kappa, which implies the shape of the Fourier amplitude spectrum of acceleration at high frequencies the method proposed in [2] is used. In this method the slope of the linear least-square fits to the high-frequency linear part of the acceleration spectra is related to the spectral decay parameter as:

$$b = -\pi\kappa \text{Log}(e) \quad (10)$$

The above equation is a result of the general functional form of the acceleration spectrum at high frequencies given as:

$$a(f) = A_0 e^{-\pi\kappa f} \quad f > f_E \quad (11)$$

where A_0 depends on source properties, epicentral distance and perhaps other factors, f is the frequency, κ is the spectral decay parameter and f_E is the frequency above which the spectral shape is indistinguishable from exponential decay[2] and always has the value above the corner frequency of the earthquakes (typically under 1.5 Hz) [2,3].

The procedure followed to determine, Q_β for 2005 Dahoeiyeh-Zarand earthquake for five selected central frequencies is shown in Figure 1. The Q_β values at each selected central frequency are derived by determining the slope of the least square fitted lines as shown in Figure 3. The determined Q_β values are tabulated in Table 3.

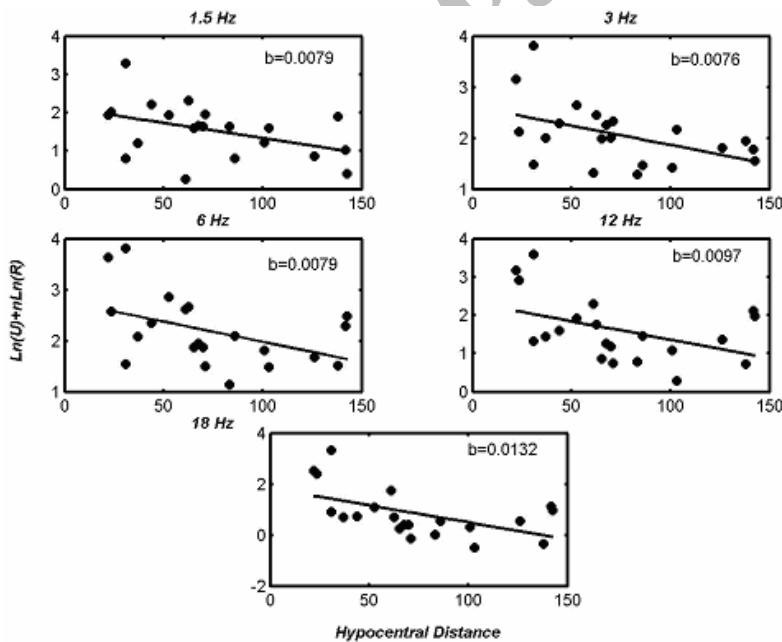


Figure 3. Estimation of the values of the quality factor, Q_β , for five frequencies selected values of the slope, b , are shown for each frequency

Using the values of Table 3, general frequency dependant form of the quality factor can be expressed as (12):

$$Q = 138 f^{0.81} \quad (12)$$

in which $Q_0 = 138$, $\alpha = 0.81$.

Table 3. Average $Q\beta$ values for the five centre frequencies.

Central frequency	$Q\beta$
1.5	169.9702
3	356.332
6	678.2824
12	1110.8
18	1222.3

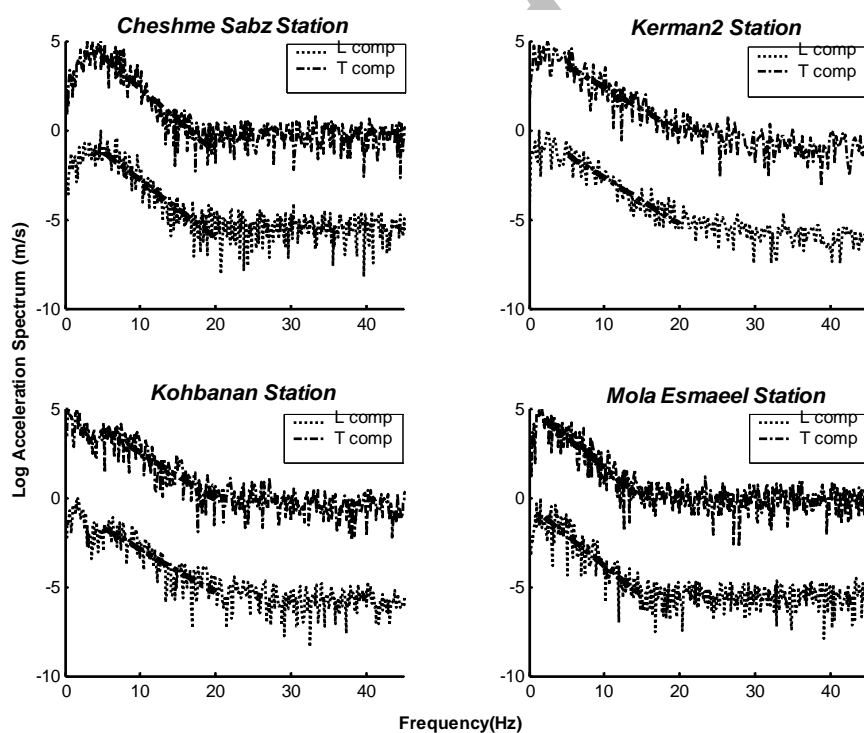


Figure 4. Examples of Fourier spectra of acceleration (horizontal components) and best fit to the high frequency parts

Figure 4 shows some examples of the Fourier amplitude spectrum, derived by calculating Fast Fourier Transform of the S portion of the recorded traces during the 2005 Dahooiyeh-Zarand main-shock. The best fitted lines to the high frequency portion of the acceleration amplitude spectrum are also shown in Figure 4.

The result of a linear correlation analysis, applied to study the dependency of kappa (κ) on epicentral distance is shown in Figure 5. The empirical relationship between epicentral distance and average kappa values, determined for two horizontal components at each station, is derived as:

$$\kappa = 0.0004r + 0.05114 \quad (13)$$

4. DISCUSSION AND CONCLUDING REMARKS

We compute the M_L using horizontal components of each accelerogram separately. For M_L computation, it is necessary to find $\Delta t(s)$ or epicentral distance (ED in Km.). For first we tried to read S and P waves arrival times directly that was possible just for 14 accelerograms, which have clear arrival times and then S-P gave up $\Delta t(s)$.

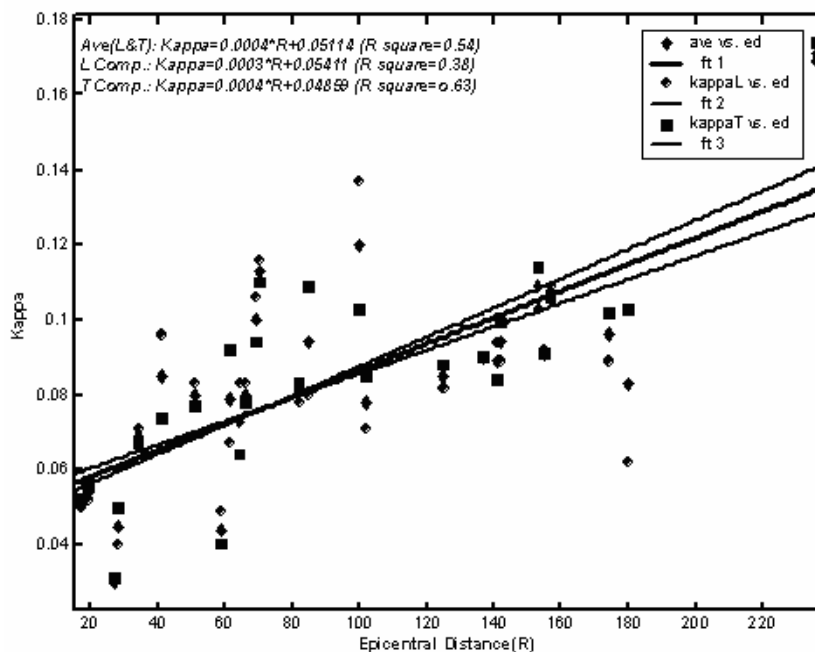


Figure 5. Dependence of spectral decay parameter on epicentral distance.

In the second method we used earthquake epicenter and stations coordinates, which yielded epicentral distances. To use these distances directly, we have been modified Eq. (2) to Eq. (14). In the first method we used Eq. (2) for M_L , and for the second method we used

Eq. (14). It was possible to use all 27 stations' accelerograms for M_L computation, since we used epicentral distances (ED).

$$M_L(j) = \text{Log}_{10} A_j(\text{mm}) + 3\text{Log}_{10}(\text{ED}(\text{km})) - 2.92 \quad (14)$$

As the path and site conditions commonly are not the same for all stations, and there is no possibility to find and apply different coefficients, this method gives up the M_L with higher standard deviation, even for the same stations' data. In this step we used the epicenter coordinates reported by BHRC, IGTU and USGS, which gave up the same results.

Finally, the accelerograms of the all possible stations are used to compute the local magnitude, and averaging the obtained values have been done for station effects minimizing.

In the next step S wave quality factor and spectral decay parameter, using 54 horizontal accelerograph components obtained during 2005 Dahooeyeh-Zarand earthquake, are determined. Based on the obtained results the frequency dependence of attenuation for shear waves can be approximated by: $Q = 138f^{0.81}$. This implies high attenuation of S wave at the studied frequency and distances.

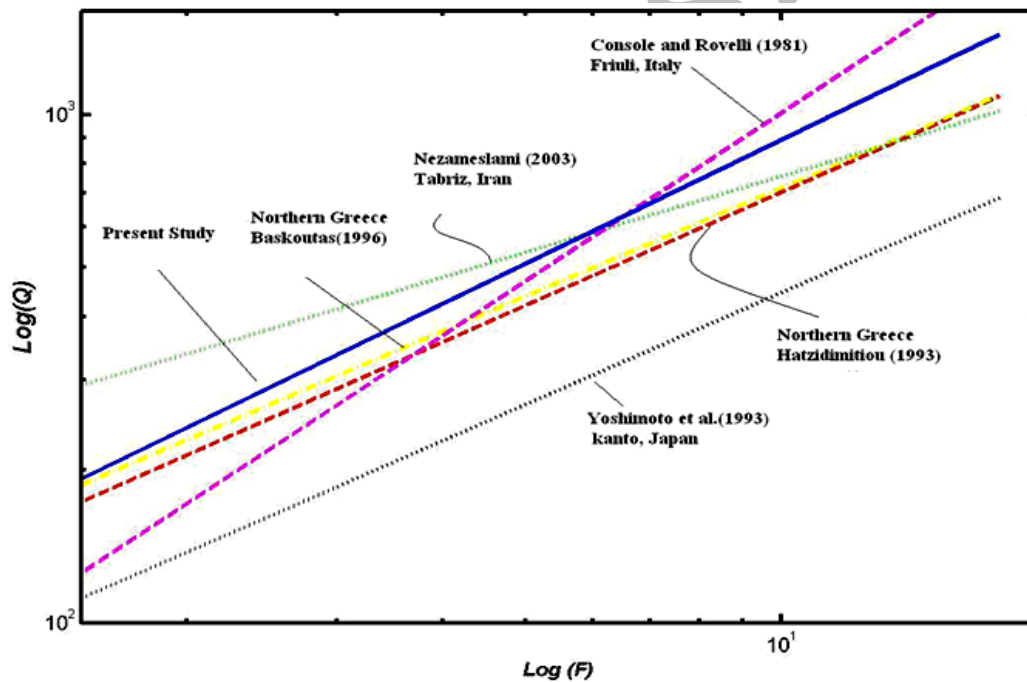


Figure 6. Comparison between the equation of attenuation and frequency that derived from the present study and the equations proposed by Hatzidimitriou (1993) [$Q_C = 128f^{0.74}$] and Baskoutas (1996) for northern Greece and central Greece [$Q_C = 140f^{0.71}$]. The attenuation of S-waves for Kanto, Japan and for frequencies 1 – 32 (Hz) from Yoshimoto et al. (1993) [$Q_\beta = 83f^{0.73}$] and Console and Rovelli (1981) for Friuli, Italy [$Q_\beta = 80f^{1.1}$]; is shown for comparison. Our proposed relation fits well within these reported values.

The variation with in the earth of Q_β controls the attenuation of S waves which has significant importance from engineering point of view; especially it has considerable application in strong ground motion seismology for this region. Q_β will vary with in the earth as a function of temperature heterogeneity because of the sensitivity of intrinsic attenuation to the pressure and temperature conditions [1,14]. Several studies have shown that for seismically active regions the range of Q and α can be considered as $\alpha > 0.4$, $Q < 300$ and for moderate to low seismicity regions we have $\alpha < 0.2$, $Q > 1000$ [15].

Comparing the obtained results with these ranges, show that the Q_β values for studied region lie in the determined range for seismically active regions which is also quite in agreement with the historical and instrumental seismicity of the region.

A number of observations have been made for the study of Q_β for different seismically active regions of the world. Our estimates, as shown graphically in Figure 6, are within the estimated ranges for different parts of the world for Q_0 and α values.

Spectral decay parameter, kappa, is a function of distance and the site condition of the station. Figure 5 shows the increasing trend of spectral decay parameter with epicentral distance which is caused due to lateral propagation. The observed scattering in kappa values, as shown in Figure 6 can be interpreted as a major contribution to kappa results from a subsurface geologic structure effect. The determined attenuation parameters in this study could be served as essential inputs for some methods to simulate strong motions for engineering applications in addition it is necessary to incorporate the given results to future seismic hazard analysis studies.

REFERENCES

1. Stein, S. and Wysession, M. *An Introduction to seismology, earthquakes and earth structure*, Blackwell, Malden, MA, USA, 2003.
2. Anderson, J.G. and Hough, S.E. A model for the shape of the Fourier amplitude spectrum of acceleration at high frequencies, *Bull. Seismol. Soc. Am.*, **74**(1984) 1969–1993.
3. Dimitriu, P. Theodulidis, N. Hatzidimitriou, P. and Anastasiadis, A. Sediment nonlinearity and attenuation of seismic waves: a study of accelerograms from Lefkas, western Greece, *Soil Dynamics and Earthquake Engineering*, **21**(2001)63-73.
4. Boore, D. M., Stephens, C.D. and Joyner, W.B. Comments on baseline correction of digital strong-motion data: examples from the 1999 Hector Mine, California, Earthquake, *Bull. Seismol. Soc. Am.*, **92**(2002)1543–1560.
5. Kanamori, H. and Jennings, P.C. Determination of local magnitude, M_L , from strong motion accelerograms, *Bull. Seismol. Soc. Am.*, **68**(1978)471-485.
6. Kanamori, H. and Anderson, D.L. Theoretical basis of some empirical relations in seismology, *Bull. Seismol. Soc. Am.*, **65** (1975)1073–1095.
7. Kanamori, H. Maechling, P. and Hauksson, E. Continuous monitoring of ground-motion parameters, *Bull. Seismol. Soc. Am.*, **89**(1999)311-316.
8. Richter, C.F. *Elementary Seismology*, W.H. Freeman, San Francisco, 1958.
9. Anderson, J. and Quaa, R., The Mexico earthquake of September 19, 1985, effect of

- magnitude on the character of strong ground motion: an example from the Guerrero Mexico strong motion network, *Earthq. Spectra*, **4**(1988)635–646.
10. Castro, R.R. Anderson, J.G. and Singh, S.K. Site response, attenuation and source spectra of S waves along the Guerrero Mexico, subduction zone. *Bull. Seismol. Soc. Am.* **80**(1990)1481-1503.
 11. Castro, R.R. Monachesi, G. Mucciareli, M. Trojani, L. and Pacor, F.P. and S-wave attenuation in the region of Marche, Italy, *Tectonophysics*, **302-1**(1999) 123-132.
 12. Castro, R.R. Monachesi, G. Trojani, L. Mucciareli, M. and Frapiccini, M. An attenuation study using earthquakes from the 1997 Umbria– Marche sequence, *J. Seismol.* **6**(2002)43–59.
 13. Anderson, J. and Lei, Y. Nonparametric description of peak acceleration as a function of magnitude, distance and site in Guerrero Mexico. *Bull. Seismol. Soc. Am.* **84**(1994)1003-1017.
 14. Lay, T. and Wallace, T.C. *Modern Global Seismology*, International Geophysics Series, Academic Press, 1995.
 15. Martinov, V.G. Vernon, F.L. and Mellors, R.J. High frequency attenuation in the crust and upper mantle of the northern Tien Shan, *Bull. Seism. Soc. Am.* **89**(1999) 215-238.

Archive of SID